A High-Frequency Beamforming Channel for Ultrasound Stimulation and Ultrasonic Powering

Rivandi, Hassan; Ghosh, Ishaan; Costa, Tiago L.

DOI
10.1109/BioCAS54905.2022.9948550

Publication date
2022

Document Version
Final published version

Published in
Proceedings of the 2022 IEEE Biomedical Circuits and Systems Conference (BioCAS)

A High-Frequency Beamforming Channel for Ultrasound Stimulation and Ultrasonic Powering

Hassan Rivandi
Microelectronics department
Delft University of Technology
Delft, The Netherlands
h.rivandi@tudelft.nl

Ishaan Ghosh
Microelectronics department
Delft University of Technology
Delft, The Netherlands
igishaan1996@gmail.com

Tiago L. Costa
Microelectronics department
Delft University of Technology
Delft, The Netherlands
t.m.l.dacosta@tudelft.nl

2022 IEEE Biomedical Circuits and Systems Conference (BioCAS) | 978-1-6654-6917-3/22/$31.00 ©2022 IEEE | DOI: 10.1109/BioCAS54905.2022.9948550

***Abstract*—New non-imaging ultrasound applications, such as ultrasound stimulation and ultrasonic power transfer, need sub-millimeter volumetric spatial resolution, electronically control of the focal spot location, high ultrasound intensity, and a tiny form factor. Satisfying these requirements demands a high-frequency phased array ultrasound transducer. On the other hand, the pitch size in a phased array must be half of the sound wavelength to avoid grating lobes in the ultrasound beam profile. In other words, higher frequency results in a smaller available area to implement a high-voltage electronics beamforming channel. While prior efforts have reached a maximum frequency of 8.3 MHz, this work utilizes a low area high-voltage level shifter coupled with optimum phase wrapping to present two 15 MHz and 12 MHz pixel-level pitch-matched beamforming channels that deliver 20 V and 36 V to the ultrasound transducer load, respectively. Furthermore, the phase of the output is programmable with 3-bits resolution that allows fine control of focal spot location. The proposed beamforming channels have been implemented in 0.18-µm BCD technology and consume 960 μA and 1.23 mA from 20 V and 36 V power supplies, respectively.**

***Index Terms*—ultrasound phased array, ultrasound transducers, ultrasound stimulation, ultrasonically powered, ultrasound neuromodulation, phased array beamformer, high-voltage beamforming channel.**

I. Introduction

Emerging sub-mm scale ultrasound (US) biomedical applications, such as ultrasound neuromodulation [1], [2] and ultrasonic power transfer for medical implants [3], [4], demands new US transmitters, Fig. 1. Opposing to the traditional ultrasound imaging systems [5], these applications require the development of 2D ultrasound phased array transmitters that can focus continuous ultrasound waves with peak acoustic intensities above 1 W/cm^2 and pulse duration in the millisecond range [6]. In addition, improvements in the volumetric spatial resolution of the produced focal spot should accompany the ever-shrinking size of ultrasonically powered implants, which can be as low as 0.065 mm^3 [7] for shallow implants, and match the micrometer scale of neurons in both deep and cortical circuits. These specifications, in turn, demand the ultrasound frequencies above the typical 3-5 MHz used in ultrasound imaging [8], [9]. These requirements impose severe constraints on the design of 2D phased array electronics, both in the reduced pixel available area imposed by the half-wavelength two-dimensional pitch and in delivering high voltages to the transducer elements.

In order to overcome these limitations, two 2D phased array ultrasound transducers have been introduced in [10], [11]. However, despite achieving high ultrasound intensity and deep penetration depth, the relatively low ultrasound frequencies of 1 and 3.4 MHz limit the volumetric focal spot resolution to cubic-mm range. The generated focal spot's size is far from the desired resolution for precise neuromodulation or powering micro-scale medical implants. [12] has tried to improve the focal spot resolution by pushing the frequency to 8.3 MHz. However, the ultrasound intensity at the focal spot is less than 100 KPa, while both US neuromodulation and US power transfer require an ultrasound pressure in the range of MPa. This paper proposes two pixel-level pitch-matched high voltage beamforming channels that pave the way for implementing a high-frequency 2D phased array ultrasound transducer. While the proposed beamforming circuits can drive the ultrasound transducer elements with continuous pulses of 20 V and 36 V, respecting the half-wavelength 2D pixel area avoids the generation of grating lobes in the US beam profile. Moreover, controlling the phase of the output signal with 3-bits resolution enables fine control of the focal spot location.

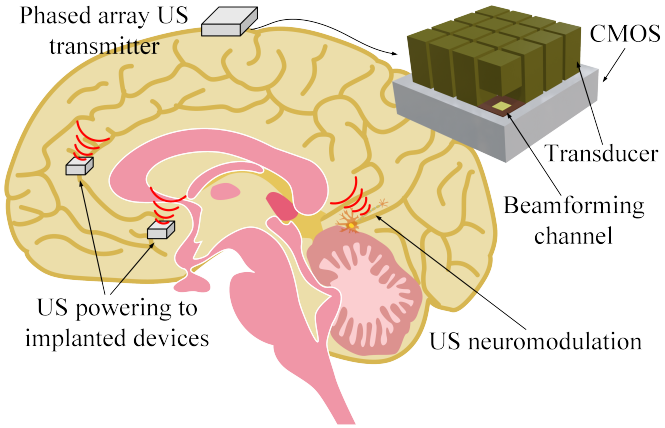

Fig. 1: A conceptual ultrasound transmitter performing both ultrasound neuromodulation and powering implanted devices in the human brain.

The organization of the rest of the work is as follows: Section II discusses the system design of the corresponding 2D phased array US transducer. Then, Section III describes the circuit design of the proposed beamforming channel. Section IV presents the experimental electrical characterization of the CMOS chip, and Section V concludes the paper.

II. System Design

In a 2D phased array US transducer, as depicted in Fig. 2, a CMOS chip drives the transducer elements with a given

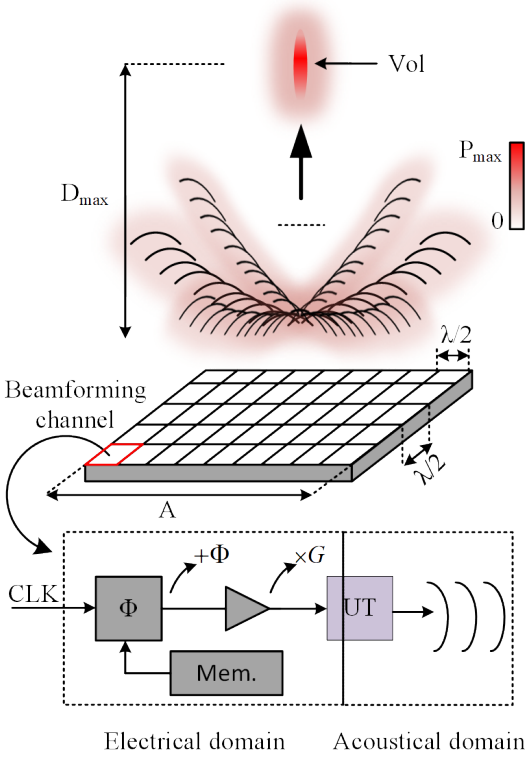

Fig. 2: Principal properties of a 2D phased array ultrasound transducer.

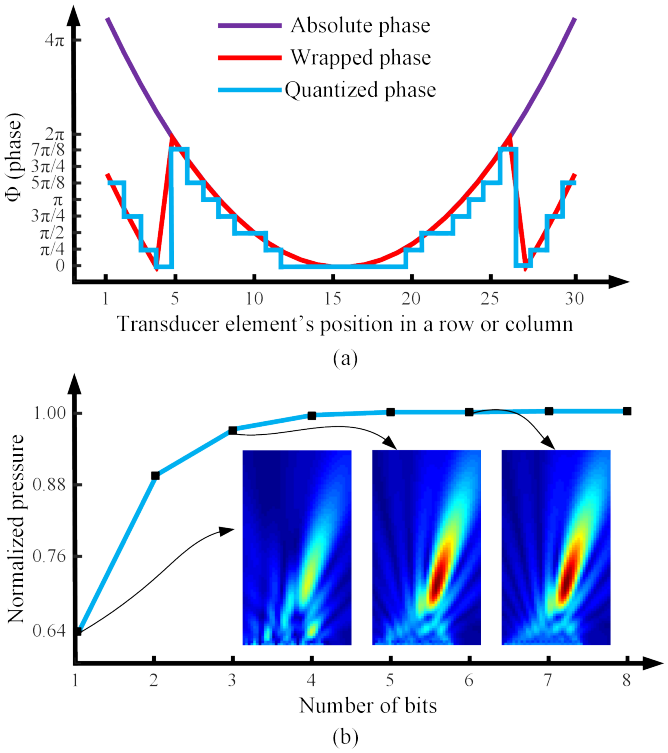

Fig. 3: (a) Phase of transducer's elements in a row or column. (b) Influence of phase quantization on focal spot properties of a 20×20 US array at depth of 2 mm and steering angle of 15°.

frequency of f_{US}, representing the resonance frequency of the US transducers, and the specific phase of Φ. On the transducer array side, an array of $N \times N$ US transducer with the inter-element pitch of d generates ultrasound waves to form a steerable focal spot.

Designing a phased array for non-imaging applications demands a comprehensive investigation of the relationship between the aforementioned characteristics. The most important variable affecting focal pressure and volumetric resolution is the frequency, f_{US}. [12] has shown that increasing the frequency leads to finer focal spot dimensions as well as higher phased array gain. In addition, expanding the number of elements, N, has a direct influence on improving focal spot resolution and gain [13]. In order to avoid grating lobes in the beam profile and achieve maximum steering capability, d must equal sound half-wavelength, $\lambda/2$. In this regard, increasing the frequency, in other words, decreasing λ, results in a smaller pitch size. Therefore, the available area for implementing a pixel-level pitch-matched circuit decreases with frequency.

In order to change the focal spot location electronically, phasing of the US transducers is required. However, wrapped phased can be used instead of absolute phase in non-imaging applications, as shown in Fig. 3(a) [12]. Furthermore, phase quantization prevents complex circuits in the beamformer while allowing precise steering. Fig. 3(b) depicts the influence of phase quantization on the normalized output pressure through k-Wave simulations [14]. It is clear that normalized focal pressure and volumetric spatial resolution do not significantly improve for phase resolution above three bits. In this regard, this work implemented 3-bits beamforming channels to avoid over designing as same the prior works [11], [12].

According to the discussion in this section, increasing N and frequency improve volumetric resolution and phased array gain. However, increasing N leads to higher occupied area, which complicates implementing a wearable device further. In this regard, this work aims to design a high-frequency beamforming channel that fulfills the high-frequency requirements of the target applications. Moreover, generated US pressure is proportional to the driving voltage; thus, achieving the necessary focal spot pressure requires high driving voltages [11]. Therefore, a 36 V beamforming channel is designed that occupies only 60×60 μm^2. Utilizing this beamformer, a 12.5 MHz pixel-level pitch-matched 2D phased array US transducer can be implemented. To push the frequency higher, another 50×50 μm^2 beamforming circuit channel is implemented that can drive the transducer elements up to 20 V and 3-bits phasing.

III. Electronic Circuit Design

The electronics circuit of a 2D phased array transmitter, as illustrated in Fig. 4, consists of course digital-to-time converter (DTC), clock buffer tree, and beamforming channels. Course DTC transforms an external clock into delayed clocks with specific timing resolution [15]. Then, a clock buffer tree distributes these clock among beamforming channels. This paper presents two beamforming channels that deliver 36 V and 20 V to the transducer elements. As depicted in Fig. 5, the 36 V beamforming channel includes a multiplexer, 3-bits shift register, 1-bit DTC, a 1.8-5 V level shifter, a high-voltage

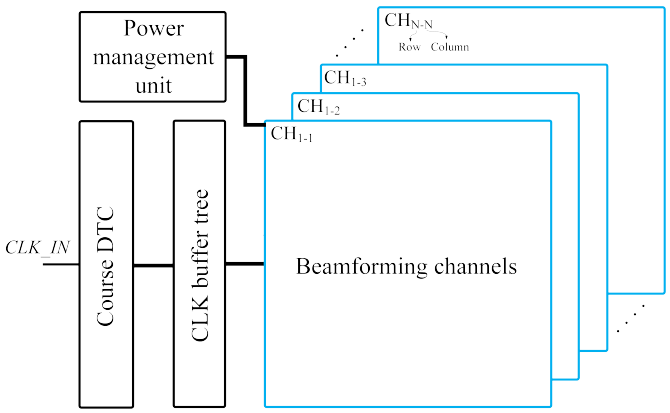

Fig. 4: System architecture of the electronics circuit of a 2D phased array US transducer.

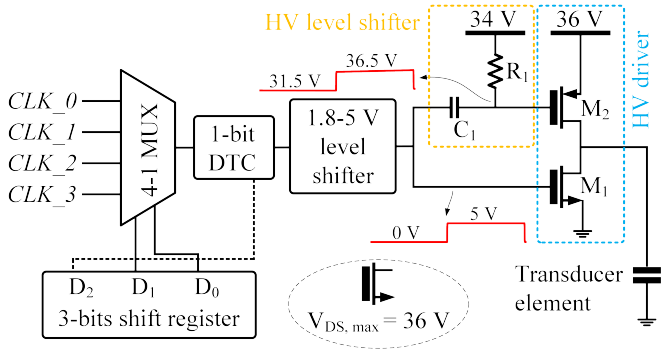

Fig. 5: The schematic of proposed 36 V beamforming channel in 60×60 μm^2.

level shifter, and an HV driver. The shift register stores the data corresponding to the phase of the beamformer. Based on this data, multiplexer passes one of the course DTC's clocks to 1-bit DTC. The fine DTC is implemented utilizing a simple inverter and a 2-1 multiplexer that selects either the input clock or the inverted of input clock. In the next step, the level of the clock shifts to 5 V, using a level shifter, to drive HV transistors. While the clock is directly connected to the gate of HV NMOS transistor, a high voltage level shifter is required to change the level of the voltage to 36 V, allowing to turn on and off the HV PMOS transistor. The last block is the HV driver that is implemented using a simple HV inverter to drive the transducer element.

Several architectures have been presented in the literature to implement an HV level shifter. However, either they have utilized HV transistors [16] that occupy a large area or used low voltage transistors in deep-NW layer [17] that require large separation distance. [11] has utilized an high-pass RC filter parallel with a diode to implement an HV level shifter. To save area, we have used this architecture without the diode, while C_1 and R_1 are implemented using metal-oxide-metal (MOM) capacitor on top of the active circuit and poly resistor, respectively. The value of C_1 and R_1 are selected enough large (i.e., 400 fF and 800 KΩ) to push the corner frequency of the high-pass filter close to DC frequency. This may increase the power dissipation from 5 V power supply that is ignorable in compression with the power consumption from HV power

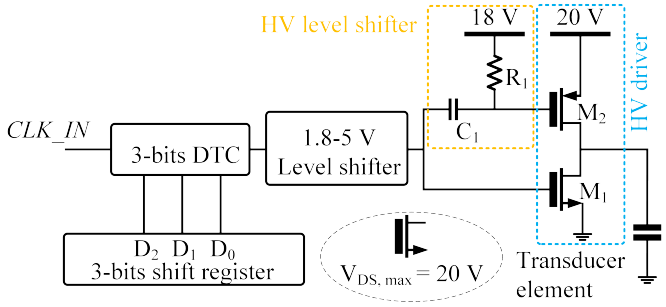

Fig. 6: The schematic of proposed 20 V beamforming channel in 50×50 μm^2.

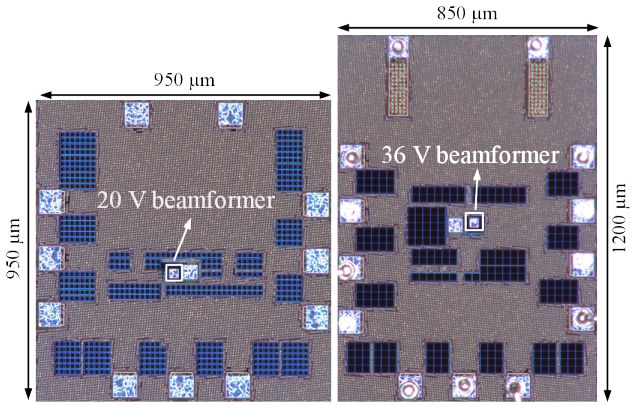

Fig. 7: The micrograph of the pixel-level pitch-matched beamforming channels.

supply. Furthermore, Connecting the top connection of R_1 to 36 V results in a pulse that changes between 33.5-38.5 V. The overshoot voltage may damage the HV PMOS transistor. To overcome this problem, we connected the resistor to 34 V, leading to a shifted pulse of 31.5-36.5 V. The external power management block generates 34 V power supply from the 36 V power supply in such a way that the source-gate voltage of the HV PMOS transistors never exceeds 5 V.

As discussed in the previous section, higher frequency and driving voltage leads to higher US pressure in the focal spot. However, employing large HV transistors increases the beamforming channel area, which limits the frequency to avoid the appearance of grating lobe in the US beam profile. To push the frequency higher, a 15 MHz 20 V beamforming channel is designed by utilizing 20 V HV transistors that occupy smaller area compared with 36 V HV transistors. As shown in Fig. 6, this circuit uses a 3-bits DTC to generate a delayed clock from an external clock (i.e., CLK_IN) inside the channel. Then, the level of the delayed clock is shifted to 5 and 20 V to drive the HV transistors.

IV. Measurements Results

The proposed beamforming channels have been realized in TSMC 0.18-µm HV BCD technology. The chip micrograph is shown in Fig. 7. While the 36 V beamforming channel is implemented in an area of 60×60 μm^2, the total area, including pad and pad drivers, occupies 850×1200 μm^2. While HV transistors are responsible for 70% of the occupied area, LV circuits and HV level shifter occupy 23% and 7%

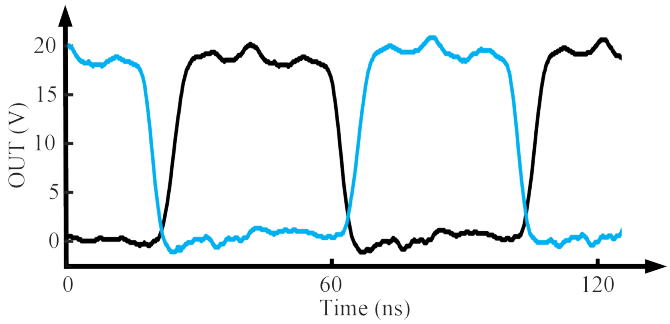

Fig. 8: Measured output waveform of 36 V beamforming channel for two delay settings of ”000” and ”100”.

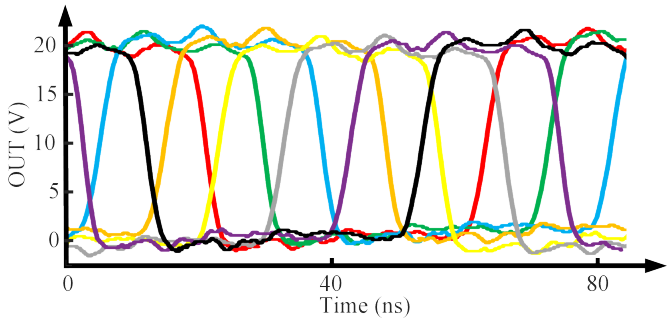

Fig. 9: Measured output waveform of 20 V beamformer for different phase configurations.

of the pixel area. The 20 V beamforming channel occupies 950×950 μm^2, although the beamformer is implemented in a square of 50×50 μm^2.

To analyze the performance of the 36 V beamformer, four external 12.5 MHz delayed clocks were applied to the beamformer. The beamformer selects one of the delayed clocks according to the two least significant bits (LSBs) stored in the shift registers. Then, the most significant bit (MSB) determines whether the clock or inverted clock can pass to the level shifter. Different configuration was applied to evaluate the circuit's functionality. The measurement results showed that the maximum differential non-linearity (DNL) is 3 ns which is less than half of the timing resolution (i.e., 5 ns). Fig. 8 depicts the output of 36 V beamformer when two different configurations of ”000” and ”100” were applied to the shift registers. However, the voltage limit of available high-voltage probes limited the applied voltage to 20 V during the measurements. The beamforming channel consumes 1.23 mA from 36 V power supply, while the power consumption from low-voltage supplies is negligible.

In the next step, the functionality of the 20 V beamformer was evaluated by applying a 60 MHz external clock to the circuit. Then, the beamformer delivers a 15 MHz 20 V pulse to the load with a 3-bits programable phase. The output signal for different delay settings is shown in Fig. 9. Since linearity is the most important characteristic of time-based circuits [18], the delay transfer function of the proposed circuit was measured, Fig. 10. The maximum DNL of the transfer curve is 2 ns that is less than half of timing resolution (i.e., 4.2 ns). The proposed beamforming channel consumes 960 μA from 20 V power supply.

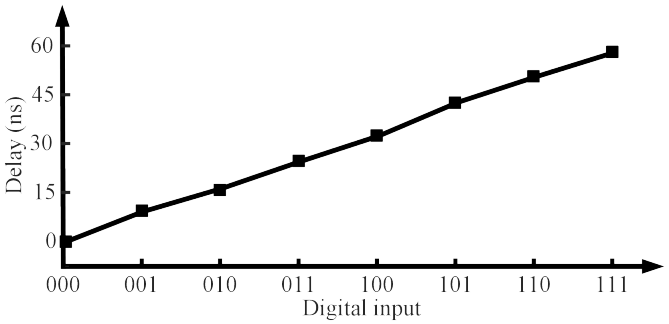

Fig. 10: Delay transfer function of 20 V beamforming channel.

TABLE I: COMPARISON OF THIS WORK WITH STATE-OF-THE-ART BEAMFORMING CHANNELS

	[9]	[11]	[12]	This work
Application	Imaging	Neuromodulation	Neuromodulation	Neuromodulation
Technology	0.25-μm HV	0.18-μm HV	0.18-μm LV	0.18-μm HV
Frequency (MHz)	5	3.4	8.4	12 @ 36 V 15 @ 20 V
Pitch (μm)	250 (1.67λ)	250 (0.57λ)	135 (0.91λ)	60 @ 36 V 50 @ 20 V (0.5λ)
Out Vpp (V)	50	60	5	20 and 36
Phase quantization	10-bits	4-bits	6-bits	3-bits

Table I shows this work against state-of-the-art beamforming circuits for non-imaging US applications. The proposed beamformer delivers up to 36 V to the US transducer while occupying only 60×60 μm^2. In this regard, the proposed beamformer can be utilized in a high-frequency 2D phased array transducer, capable of generating programable high-voltage pulses. In terms of phase quantization, this work has shown that 3-bits phase quantization, either at the pixel or at the periphery level, can maximize focal pressure and spatial resolution, thus avoiding more area and power consuming circuits as in [11] and [12].

V. CONCLUSIONS

This paper presents two beamforming channels that pave the way for implementing a high-frequency phased array US transducer. At first, a system design analysis was established to investigate the relationship between frequency, driving voltage, and US parameters. K-Wave simulations showed that 3-bits phase quantization can steer the ultrasound beam without affecting volumetric spatial resolution and US intensity in the focal spot. In this regard, this work designed and realized two 36 V and 20 V beamformer channels in 60×60 μm^2 and 50×50 μm^2, respectively. The 36 V beamforming channel achieves 3-bits quantization through 1-bit in-channel phasing and receiving four delayed clocks from course DTC. On the other hand, 20 V beamforming channel does 3-bit quantization inside the channel. The measurement results proved the performance of the proposed beamforming channels in terms of driving capability up to 20 V and 3-bits phasing with a maximum DNL of half of the timing resolution.

REFERENCES

[1] W. Legon, T. F. Sato, A. Opitz, J. Mueller, A. Barbour, A. Williams, and W. J. Tyler, "Transcranial focused ultrasound modulates the activity of primary somatosensory cortex in humans," *Nature Neuroscience*, vol. 17, no. 2, p. 322–329, 2014.

[2] M. E. Downs, S. A. Lee, G. Yang, S. Kim, Q. Wang, and E. E. Konofagou, "Non-invasive peripheral nerve stimulation via focused ultrasound in vivo," *Physics in Medicine & amp; Biology*, vol. 63, no. 3, p. 035011, 2018.

[3] J. Vo, T. C. Chang, K. I. Shea, M. Myers, A. Arbabian, and S. Vasudevan, "Assessment of miniaturized ultrasound-powered implants: An in vivo study," *Journal of Neural Engineering*, vol. 17, no. 1, p. 016072, 2020.

[4] A. Rashidi, K. Laursen, S. Hosseini, H.-A. Huynh, and F. Moradi, "An implantable ultrasonically powered system for optogenetic stimulation with power-efficient active rectifier and charge-reuse capability," *IEEE Transactions on Biomedical Circuits and Systems*, vol. 13, no. 6, pp. 1362–1371, 2019.

[5] M. Tan, C. Chen, Z. Chen, J. Janjic, V. Daeichin, Z.-Y. Chang, E. Noothout, G. van Soest, M. D. Verweij, N. de Jong, and et al., "A front-end ASIC with high-voltage transmit switching and receive digitization for 3-D forward-looking intravascular ultrasound imaging," *IEEE Journal of Solid-State Circuits*, vol. 53, no. 8, p. 2284–2297, 2018.

[6] J. Blackmore, S. Shrivastava, J. Sallet, C. R. Butler, and R. O. Cleveland, "Ultrasound neuromodulation: A review of results, mechanisms and safety," *Ultrasound in Medicine & amp; Biology*, vol. 45, no. 7, p. 1509–1536, 2019.

[7] C. Shi, T. Costa, J. Elloian, Y. Zhang, and K. L. Shepard, "A 0.065-mm^3 monolithically-integrated ultrasonic wireless sensing mote for real-time physiological temperature monitoring," *IEEE Transactions on Biomedical Circuits and Systems*, vol. 14, no. 3, p. 412–424, 2020.

[8] C. Chen, Z. Chen, D. Bera, S. B. Raghunathan, M. Shabanimotlagh, E. Noothout, Z.-Y. Chang, J. Ponte, C. Prins, H. J. Vos *et al.*, "A front-end ASIC with receive sub-array beamforming integrated with a 32 $\times$ 32 PZT matrix transducer for 3-D transesophageal echocardiography," *IEEE Journal of Solid-State Circuits*, vol. 52, no. 4, pp. 994–1006, 2017.

[9] A. Bhuyan, J. Choe, B. Lee, I. Wygant, A. Nikoozadeh, O. Oralkan, and B. Khuri-Yakub, "Integrated circuits for volumetric ultrasound imaging with 2-D cmut arrays," *IEEE Transactions on Biomedical Circuits and Systems*, vol. 7, no. 6, pp. 796–804, 2013.

[10] Z. Zhang, M. Su, F. Li, R. Liu, R. Cai, G. Li, Q. Jiang, H. Zhong, T. R. Shrout, S. Zhang *et al.*, "New Sm-PMN-PT ceramic-based 2-D array for low-intensity ultrasound therapy application," *IEEE Transactions on Ultrasonics, Ferroelectrics, and Frequency Control*, vol. 67, no. 10, pp. 2085–2094, 2020.

[11] C. Seok, O. J. Adelegan, A. Ö. Biliroğlu, F. Y. Yamaner, and Ö. Oralkan, "A wearable ultrasonic neurostimulator—part II: A 2D CMUT phased array system with a flip-chip bonded ASIC," *IEEE Transactions on Biomedical Circuits and Systems*, vol. 15, no. 4, pp. 705–718, 2021.

[12] T. Costa, C. Shi, K. Tien, J. Elloian, F. A. Cardoso, and K. L. Shepard, "An integrated 2D ultrasound phased array transmitter in CMOS with pixel pitch-matched beamforming," *IEEE Transactions on Biomedical Circuits and Systems*, vol. 15, no. 4, pp. 731–742, 2021.

[13] T. Costa, C. Shi, K. Tien, and K. L. Shepard, "A CMOS 2D transmit beamformer with integrated PZT ultrasound transducers for neuromodulation," in *IEEE Custom Integrated Circuits Conference (CICC)*. IEEE, 2019, pp. 1–4.

[14] "k-wave," 2017. [Online]. Available: http://www.k-wave.org/

[15] H. Rivandi, S. Ebrahimi, and M. Saberi, "A low-power rail-to-rail input-range linear delay element circuit," *AEU - International Journal of Electronics and Communications*, vol. 79, pp. 26–32, 2017.

[16] M. Tan, E. Kang, J.-S. An, Z.-Y. Chang, P. Vince, T. Mateo, N. Sénégond, and M. A. Pertijs, "A 64-channel transmit beamformer with$\pm$30-V bipolar high-voltage pulsers for catheter-based ultrasound probes," *IEEE Journal of Solid-State Circuits*, vol. 55, no. 7, pp. 1796–1806, 2020.

[17] A. Banuaji and H.-K. Cha, "A 15-V bidirectional ultrasound interface analog front-end IC for medical imaging using standard CMOS technology," *IEEE Transactions on Circuits and Systems II: Express Briefs*, vol. 61, no. 8, pp. 604–608, 2014.

[18] H. Rivandi, F. Shakibaee, and M. Saberi, "A 6-bit 100 MS/s fully-digital time-based analog-to-digital converter," in *27th Iranian Conference on Electrical Engineering (ICEE)*. IEEE, 2019, pp. 412–415.